Article:
Knox, CS, Morrison, C, Herling, F et al. (5 more authors) (2017) Partial hybridisation of electron-hole states in an InAs/GaSb double quantum well heterostructure. Semiconductor Science and Technology, 32 (10). 104002. ISSN 0268-1242

https://doi.org/10.1088/1361-6641/aa827e

Partial hybridisation of electron-hole states in an InAs/GaSb double quantum well heterostructure

C. S. Knox[1,2], C. Morrison[1,3], F. Herling[1,4], D. A. Ritchie[5], O. Newell[2], M. Myronov[2], E. H. Linfield[2] and C. H. Marrows[1]

[1]School of Physics and Astronomy, University of Leeds, Leeds LS2 9JT, United Kingdom

[2]School of Electronic and Electrical Engineering, University of Leeds, Leeds LS2 9JT, United Kingdom

[3]Department of Physics, University of Warwick, Coventry CV4 7AL, United Kingdom

[4]Novel Materials Group, Institut für Physik, Humboldt-Universität zu Berlin, 12489 Berlin, Germany

[5]Cavendish Laboratory, University of Cambridge, Madingley Road, Cambridge CB3 0HE, United Kingdom

ABSTRACT

InAs/GaSb coupled quantum well heterostructures are important semiconductor systems with applications ranging from spintronics to photonics. Most recently, InAs/GaSb heterostructures have been identified as candidate two-dimensional topological insulators, predicted to exhibit helical edge conduction via fully spin-polarised carriers. We study an InAs/GaSb double quantum well heterostructure with an AlSb barrier to decouple partially the 2D electrons and holes, and find conduction consistent with a 2D hole gas, with an effective mass of 0.235±0.005 m_0, existing simultaneously with hybridised carriers with an effective mass of 0.070±0.005 m_0, where m_0 is the bare electron mass.

Introduction

Recently, interest in materials with topologically protected transport properties has bloomed[1]. Amongst these are quantum spin Hall insulators, otherwise known as two-dimensional topological insulators (2DTIs). These 2DTIs contain topologically non-trivial band gaps where the insulating state is topologically distinct from the vacuum. Due to this distinction, a transition region between the interior of the sample and the outside vacuum is required. In a 2DTI this takes the form of a pair of counter-propagating 1D helical edge channels running around the sample perimeter, protected from elastic backscattering by spin-momentum locking[2].

Two materials systems have been experimentally verified as 2DTIs to date, HgTe quantum wells[3,4] and InAs/GaSb coupled quantum wells[5,6,7]. In both of these structures the non-trivial topology is provided by so-called inverted band structures. In HgTe this inversion comes about through strong Dresselhaus spin-orbit coupling, which causes the top of the valence band to be more energetic than the bottom of the conduction band when the well has a width greater than a critical value. A similar scenario arises in InAs/GaSb coupled quantum wells due to the band alignment between the 2D electron gas in the InAs layer and the 2D hole gas in the GaSb layer. States in the conduction band of the InAs can hybridise with light-hole states in the GaSb valence band[8]. This coupling opens an anti-crossing gap in the dispersion relation, leading to the inverted band gap. This provides the non-trivial topology needed for a 2DTI state[9].

This unusual band-structure in the InAs/GaSb system allows heterostructures to be devised in which it is possible to adjust intentionally the level of hybridisation between the InAs and

GaSb wells by separating the two wells with an additional tunnel barrier layer. By altering the tunnel barrier thickness, one can then effectively change the coupling between the two carrier gases. Several studies also report altering the composition of the coupled quantum well system in order to make the contribution from the topologically protected edge states more distinct from residual the bulk conductivity when the system is tuned into a state where the 2DTI behaviour dominates transport[6,10,11]. However, as these studies use the magnitude of the resistance resonance at charge neutrality as a measure of quality [10,11], it is possible that the coupling between the two carrier gases is adversely affected. To demonstrate this we show that by physically separating the two quantum well structures, some of the carriers in the GaSb decouple from the hybridised states, which leads to them acting independently as a hole gas separate from the hybridised carriers.

The layer structure of the coupled quantum wells studied here is shown in Figure 1(a). The active region is composed of 15 nm InAs and 15 nm GaSb quantum wells, separated by a barrier of 2.5 nm of AlSb, and surrounded by AlSb barriers at least 50 nm thick. As the inter-layer separation between the quantum wells increases, the size of the anti-crossing gap decreases. As it does so, the anti-crossing point, where the hybridisation gap opens, decreases in k (shown in Figure 1 (b-c)). A barrier thickness of 2.5nm was chosen for this study, as it has been predicted that, at this thickness, the hybridisation gap will still be energetically significant while at the same time, it should make it easier to excite uncoupled states, highlighting their effect on transport[12]. If the barrier was much thicker (of the order of 5 nm), the hybridisation gap would close, creating a semimetallic system dominated by the high mobility carriers in InAs.

We now show that in this system there is a coexistence of hole and hybridised electron-hole states, resulting in a quantum transport behaviour that deviates from conventional 2D quantised transport behaviour and from previously observed electron-hole hybridisation in heterostructures of this class. We find that these results do not agree with the type of hybridisation seen by Suzuki et al. for a thicker barrier[13], since the hybridised plateaux do not occur at integer values of combined filling factor $|\nu_e - \nu_h|$, nor can this behaviour be explained by parallel conducting, non-interacting electron and hole gases [14], as the plateaux occur at integer fractions of the von Klitzing constant $\frac{h}{e^2}$. Rather, this deviation occurs only when we insert a 2.5nm AlSb spacer between the two quantum well layers. For intimate contact, Knez et al.[15] observe a linear increase in Hall resistance which develops into perfect even-integer quantised plateaux at high fields in similar, unbiased, structures. This behaviour signifies that transport is dominated by a single carrier type, in this case electrons. Additionally, Suzuki et al. observe for strongly hybridised quantum wells, in which the linear Hall trace develops into plateaux that occur at integer values of combined filling factor $|\nu_e - \nu_h|$, that transport is dominated by a single transport channel that contains carriers with a unified effective mass [13].

Experiment

Resistivity and Hall resistance data, measured in a square van der Pauw geometry, are shown in Figure 2. The devices are 500 µm squares, much larger than the expected length at which any possible 2DTI state would dominate transport (approx. 4 µm) [11]. As such, the behaviour reported here is attributed solely to bulk transport through the material. The contacts are 100 µm squares at each corner, and the I-V characteristics are all ohmic at 0 T. No gate bias was applied during this experiment.

At low fields, the Hall resistance is non-linear, which suggests parallel conduction channels. Shubnikov-de Haas (SdH) oscillations are observed from 2 T onwards, and a fast Fourier transform of this data (not shown) to extract the carrier density reveals that these oscillations, which are periodic in inverse field with a single frequency when disregarding Zeeman split peaks[16], are due to carriers with a density equal to the Hall carrier density of $(11.8 \pm 0.1) \times 10^{11}$ cm^{-2}. These low-field SdH oscillations were observed up to 32.4 K, as illustrated in Figure 2(c). The features did not change based on field or field sweep direction. Below 2 K, he data were acquired using a full sweep from 0 T to +12 T, then to -12 T, and finally back to 0 T. For temperatures above 2 K, the data was acquired by sweeping the magnetic field between 0 T and 5 T.

The majority carriers in this heterostructure are electrons at all temperatures, as confirmed by the sign of the Hall coefficient. However, the Hall resistance plateaux below 5 T occur at non-integer values of the von Klitzing constant. Above 4 T, Zeeman split peaks in the magnetoresistance begin to emerge, with corresponding plateaux where one would expect odd-integer filling factors from the oscillations in magnetoresistance [16].

The first integer plateau occurs for a filling factor of $\nu = 6$, and exact quantisation is present at all further filling factors up to $\nu = 3$. However, the magnetic field at which these plateaux occur is not consistent with the Hall carrier density or the low field SdH density, instead occurring at 8.7×10^{11} cm^{-2} for the $\nu = 6$ and $\nu = 3$ plateaux, and 7.9×10^{11} cm^{-2} for the $\nu = 4$ plateau. In addition to this behaviour, there is an additional $\nu = 3$ plateau, occurring at a lower carrier density of 6.7×10^{11} cm^{-2}. Exact quantisation of this plateau only occurs at the lowest

temperature measured (338 mK); the evolution of the resistance value of the plateau is plotted in figure 3. The occurrence of two quantum plateaux at the same filling factor suggests the coexistence of two states, which we assign as hybridised electron-hole states and 2D holes. We explain the reasons for this assignment in the remainder of the paper.

Analysis and Discussion

The peaks in magnetoresistance as a function of magnetic field in the low field regime may be used to calculate the effective mass m* of carriers in the conduction region by an iterative process. The analytical equation that describes Shubnikov-de Haas oscillations is[17,18]

$$\frac{\Delta\rho_{xx}(B)}{\rho_{xx}(0)} = 4\cos\left(\frac{2\pi E_F m^*}{\hbar eB}\right)\exp\left(-\frac{\pi m^* \alpha}{eB\tau_t}\right)\frac{\psi}{\sinh(\psi)}, \quad (1)$$

where E_F is the Fermi energy, $\alpha = \tau_t/\tau_q$ is the Dingle ratio, where τ_t is the transport scattering time and τ_q is the quantum scattering time, and $\psi = \frac{2\pi^2 k_B T m^*}{\hbar eB}$.

In Fig. 4 we show plots of two quantities derived from this equation that may be used to solve iteratively a pair of simultaneous equations for the effective mass and Dingle ratio[19]. These plots represent the final iteration of the solution using an iterative step of 0.005 m_0 (where m_0 is the bare electron mass). The effective mass of these carriers is found to be m* = (0.070±0.005) m_0, and the Dingle ratio is α = 14.5±0.2. This relatively high value of the Dingle ratio suggests that there is a low amount of scattering within the channel from impurities and interfaces, and that the dominant contribution is small angle scattering events due to remote impurities[18]. The solution to these simultaneous equations accurately describes the system up to 32.2 K, after which the Shubnikov-de Haas oscillations are masked by thermal effects and cannot be accurately analysed.

The effective mass of 0.070 m_0 determined from the Dingle plots is significantly different to the accepted value for InAs 2DEGs (0.032 m_0-0.046 m_0)[20,21,22,23], and so we attribute the majority transport in this structure to hybridised electron-hole states. Additionally, this effective mass aligns extremely well with the mean of the effective masses of electrons in InAs and heavy holes in GaSb at the band centre[24], which are relevant for transport. Furthermore, previous studies of the hybridised state through cyclotron resonance in a strongly hybridised system [25] and studies of the 2DTI state observed in a strongly hybridised system [6] show that the hybridised nature of this state is largely independent of temperature, demonstrated here by the fact that a model using a temperature-independent effective mass describes the data well.

In order to determine the effective mass of carriers at the additional $\nu = 3$ plateau, a different method can be employed, using the temperature dependence of the single minimum in resistivity at the plateau field (9.3 T). If we assume that the transport properties and hence the degree of scattering in the channel is temperature independent in the measured range, the effective mass m* may be calculated by evaluating the change in minimum resistivity in terms of the temperature dependent part of equation 1 only. This is a reasonable assumption for this heterostructure, given the almost temperature invariant carrier density, mobility and resistivity. Following this methodology, the equation for sheet resistance as a function of temperature becomes

$$\ln\left(\frac{R_{\min}}{T}\right) = C - \frac{2\pi^2 k_B m^*}{e\hbar B} T, \qquad (2)$$

where R_{min} is the sheet resistance mimimum at an applied magnetic field B, and C is a constant. Therefore, finding the gradient of a straight line fit to the quantity $\ln\left(\frac{R_{\min}}{T}\right)$ as a function of temperature T allows the effective mass of the carriers to be extracted. The temperature dependence of the sheet resistance minimum at 9.3 T is shown in figure 5(a), and the plot of $\ln\left(\frac{R_{\min}}{T}\right)$ against T is shown in figure 5(b). The fit to this curve (red line) gives a value for the effective mass of these carriers as $m^* = (0.235 \pm 0.005)\, m_0$, which is close to the literature value for the heavy-hole cyclotron mass near the band-edge in GaSb [26]. We measure holes, rather than uncoupled electrons, because there are more hole-states near the Fermi level that are outside the hybridisation gapped regime due to the more gradual curvature of the heavy hole band when compared to the conduction band, as illustrated in Figure 1(c).

Gating this structure would permit tuning of E_F for a constant physical spacer thickness and consequently allow study of electron-hole hybridisation and the coexisting carrier states over a wider range of carrier densities. Such studies of electron-hole hybridisation in these structures would shed new light on the topologically non-trivial anti-crossing gap, and pave the way for new topologically insulating heterostructures or be used to decouple further the bulk and protected edge states.

This work was supported by the Engineering and Physical Sciences Research Council through the Platform grant ‘Spintronics at Leeds’ (EP/M000923/1). F.H. was supported by the ERASMUS scheme of the EU.

References

[1] M. Z. Hasan and C. L. Kane, Rev. Mod. Phys. **82**, 3045 (2010).
[2] C. L. Kane, and E. J. Mele, Phys. Rev. Lett. **95**, 226801 (2005).
[3] M. König, S. Wiedmann, C. Brüne, A. Roth, H. Buhmann, L. W. Molenkamp, X.-L. Qi, S.-C. Zhang, Science **318**, 766 (2007).
[4] C. Brüne, A. Roth, H. Buhmann, E. M. Hankiewicz, L. W. Molenkamp, J. Maciejko, X.-L. Qi, and S.-C. Zhang, Nature Phys. **8**, 485 (2012).
[5] I. Knez, R. R. Du, and G. Sullivan, Phys. Rev. Lett. **107**, 136603 (2011).
[6] E. M. Spanton, K. C. Nowack, L. Du, G. Sullivan, R.-R. Du, and K. A. Moler, Phys. Rev. Lett. **113**, 026804 (2014).
[7] M. Karalic, S. Mueller, C. Mittag, K. Pakrouski, Q.-S. Wu, A. A. Soluyanov, M. Troyer, T. Tschirky, W. Wegscheider, K. Ensslin, and T. Ihn, Phys. Rev. B **94**, 241402(2016).
[8] M. J. Yang, C. H. Yang, B. R. Bennett, and B. V. Shanabrook, Phys. Rev. Lett. **78**, 4613 (1997).
[9] C. Liu, T. L. Hughes, X.-L. Qi, K. Wang, and S.-C. Zhang, Phys. Rev. Lett. **100**, 236601 (2008).
[10] C. Charpentier, S. Fält, C. Reichl, F. Nichele, A. N. Pal, P. Pietsch, T. Ihn, K. Ensslin, and W. Wegscheider, Appl. Phys. Lett. **103**, 112102 (2013).
[11] L. Du, I. Knez, G. Sullivan, and R. R. Du, Phys. Rev. Lett. **114**, 096802 (2015).
[12] J. Li *et al.*, Phys. Rev. B **80**, 035303 (2009).
[13] K. Suzuki, S. Miyashita, and Y. Hirayama, Phys. Rev. B **67**, 195319 (2003)
[14] M. A. Reed, W. P. Kirk, and P. S. Kobiela, IEEE J. Quantum Elect. **22,** 1753 (1986).
[15] I. Knez, R. R. Du, and G. Sullivan, Phys. Rev. B **81**, 201301 (2010).
[16] S.W. Hwang *et al.,* Phys. Rev. B, **48**, 15 (1993).
[17] A. Ishihara and L. Smrcka, J. Phys. C: Solid State Phys. **19**, 6777 (1986).
[18] P. Coleridge, R. Stoner, and R. Fletcher, Phys. Rev. B **39**, 1120 (1989).
[19] Y. F. Komnik, V. V. Andrievskii, I. B. Berkutov, S. S. Kryachko, M. Myronov, and T. E. Whall, Low. Temp. Phys.+ **26**, 609 (2000).
[20] C. Petchsingh *et al.*, Semicond. Sci. Tech. **22**, 194 (2007)
[21] D. Grundler, Phys. Rev. Lett. **84**, 6074 (2000)
[22] J. Luo *et al.*, Phys. Rev. B **41**, 7685 (1990)
[23] M. Marcinkiewicz *et al.*, J. Phys. Conf. Ser. **647**, 012037 (2015).
[24] C. Petchsingh *et al.*, Physica E **12**, 289 (2002)
[25] T.P. Marlow *et al.*, Phys. Rev. Lett., **82**, 11, (1999).
[26] I. Vurgaftman, J. R. Meyer, and L. R. Ram-Mohan, J. Appl. Phys. **89**, 5815 (2001).

FIGURES

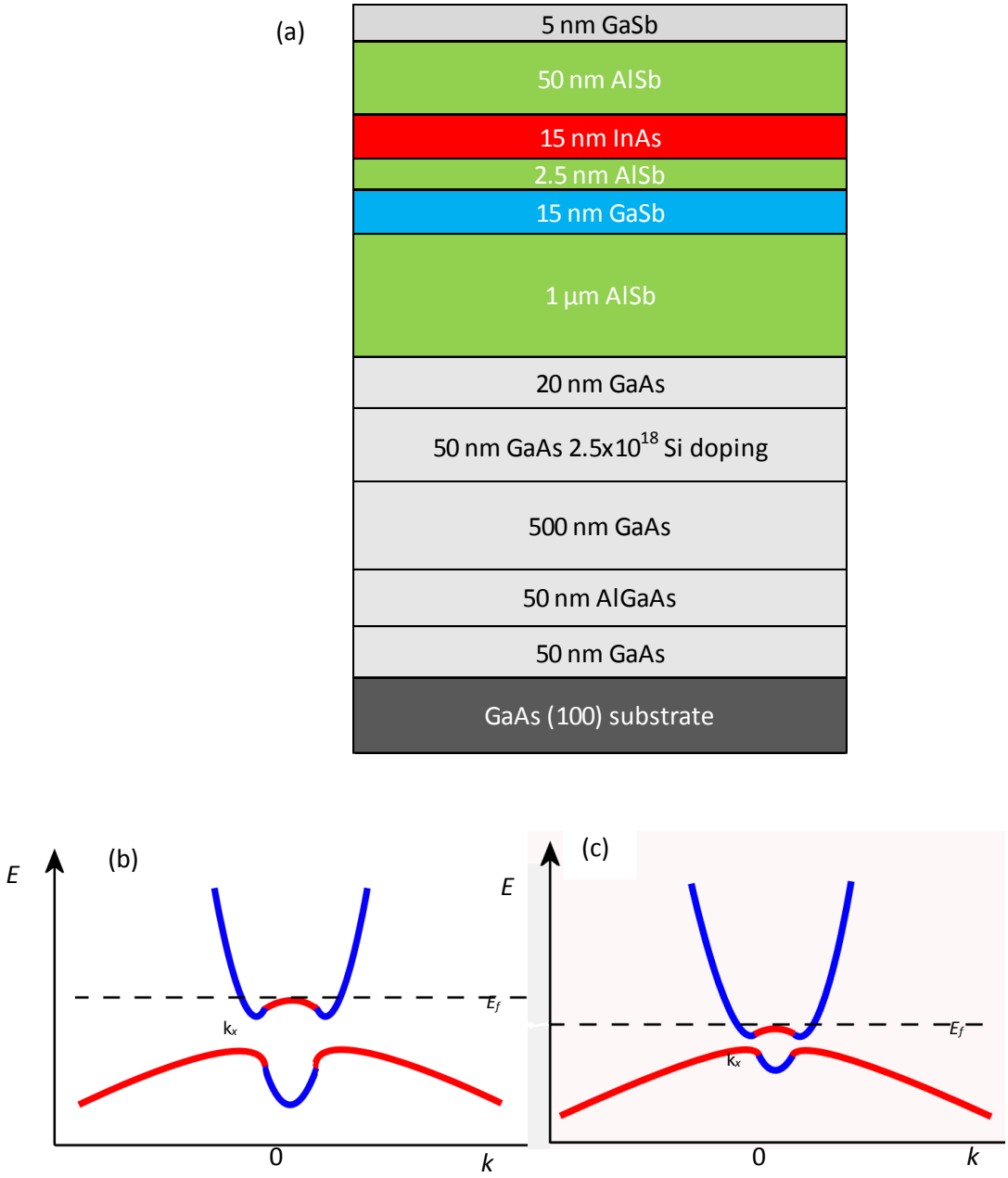

Figure 1:(a) Schematic diagram of the layer structure for the wafer that was grown by molecular beam epitaxy (MBE) onto a GaAs (100) substrate. The nominal active transport region is indicated by the red and blue sections (InAs and GaSb quantum well epilayers separated by a thin AlSb barrier). (b) Expected dispersion relation for an InAs/GaSb quantum well without an inter-layer AlSb barrier. (c) The same system but with an inter-layer AlSb barrier inserted. In both cases the anti-crossing point is indicated by k_x

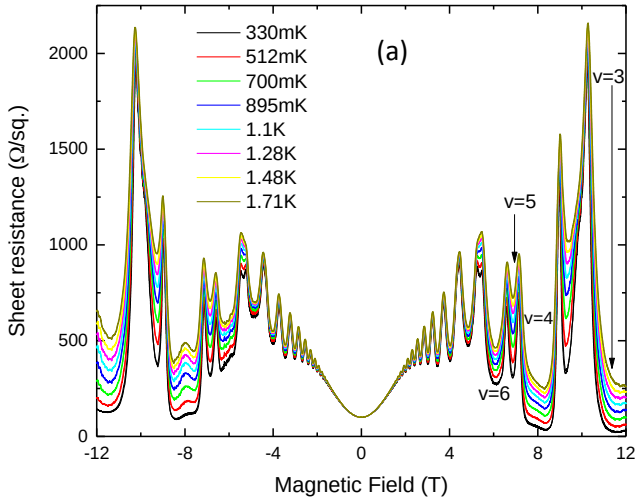
330mK
512mK
700mK
895mK
1.1K
1.28K
1.48K
1.71K
(a)
v=3
v=5
v=4
v=6
Sheet resistance (Ω/sq.)
Magnetic Field (T)

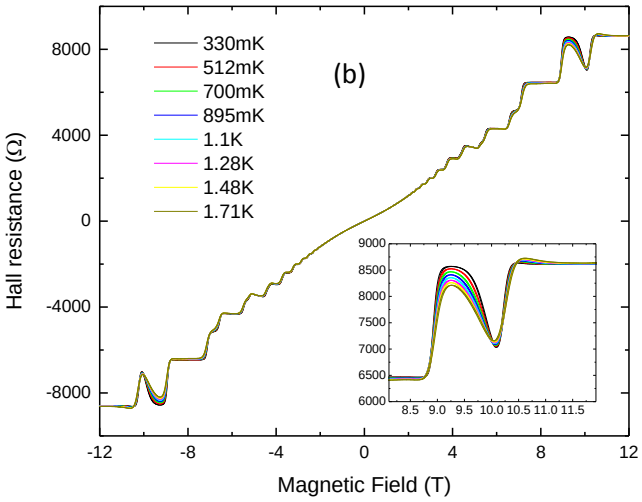
330mK
512mK
700mK
895mK
1.1K
1.28K
1.48K
1.71K
(b)
Hall resistance (Ω)
Magnetic Field (T)

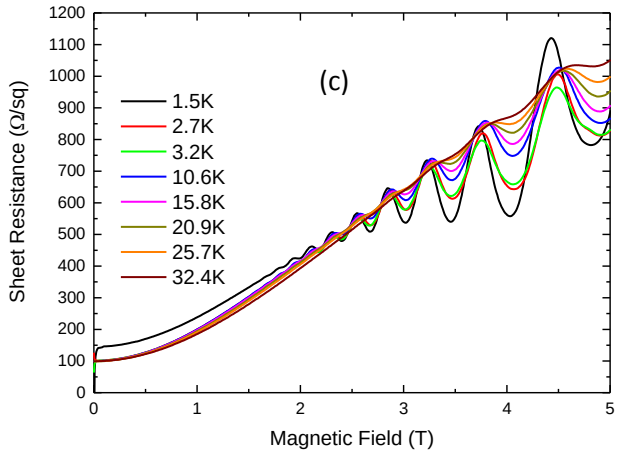
1.5K
2.7K
3.2K
10.6K
15.8K
20.9K
25.7K
32.4K
(c)
Sheet Resistance (Ω/sq)
Magnetic Field (T)

Figure 2: (a) Magnetoresistance measurements between 0.33 K and 1.7 K up to a magnetic field of 12 T, showing Shubnikov-de Haas oscillations. The behaviour observed above 8 T cannot be explained by conductivity oscillations in a single 2D electron channel. (b) Hall resistance for the same measurement conditions. The feature at 9.3 T (magnified in the inset) corresponds to an integer filling factor but occurring at a lower field than expected, suggesting electron-hole hybridisation is present. (c) Magnetoresistance measurements between 1.5 K and 32.4 K up to a magnetic field of 5 T, showing Shubnikov-de Haas oscillations, illustrating how the oscillations evolve with temperature. The behaviour shown here is typical of transport dominated by a single carrier type.

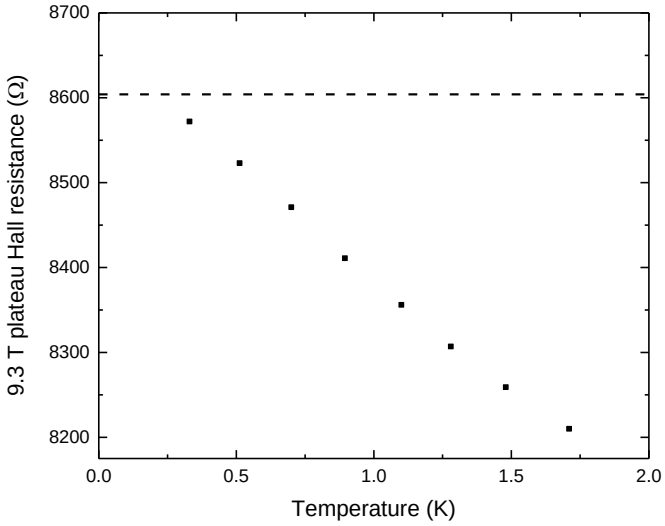

Figure 3: Hall resistance plateau at 9.3 T as a function of temperature. The value approaches $h/3e^2$ = 8604 Ω (marked by the dashed horizontal line) as the temperature is decreased. The temperature dependence is more pronounced than for the other quantised plateaux, which are well-defined at all measurement temperatures.

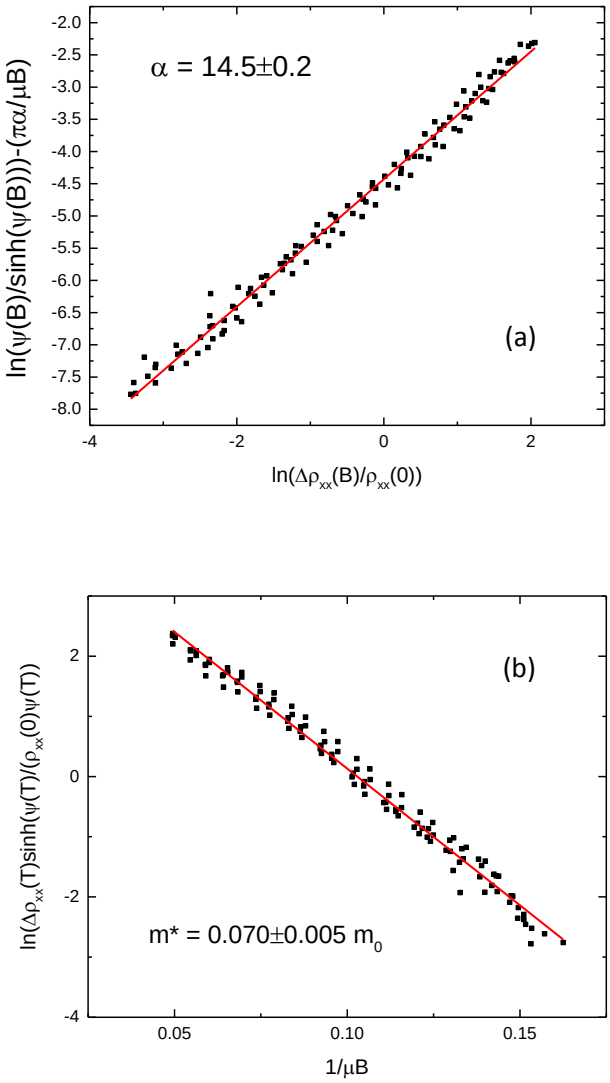

Figure 4: Plots of quantities used to solve the equation for Shubnikov-de Haas oscillations, allowing determination of (a) the Dingle ratio α and (b) the effective mass m^*. The Dingle ratio corresponds to a quantum lifetime of 0.12 ps, using the transport lifetime of 1.8 ps determined from the Hall mobility of 45,000 $cm^2V^{-1}s^{-1}$ at a temperature of 1.8 K.

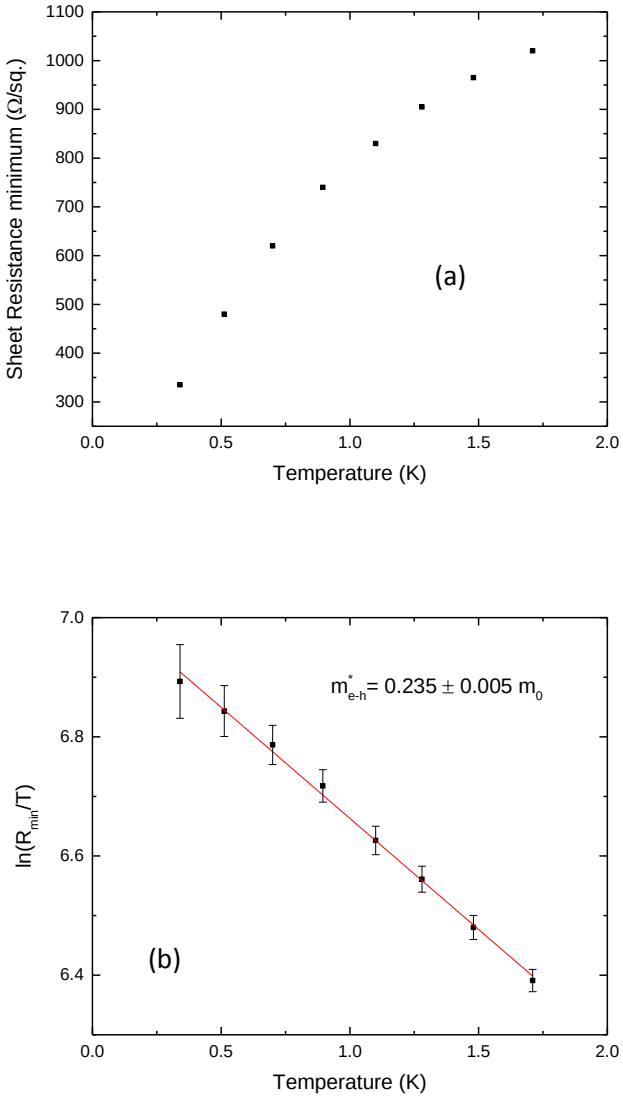

Figure 5: (a) Resistance mimimum for hybridised electron-hole states at the $\nu = 3$ filling factor as a function of temperature. (b) Plot of the natural logarithm of the ratio of the resistance minimum and temperature. A linear fit to the data allows the effective mass of the hybridised carriers (0.235±0.005) m_0 to be determined.